

Aberrant Processing of the WSC Family and Mid2p Cell Surface Sensors Results in Cell Death of *Saccharomyces cerevisiae* O-Mannosylation Mutants

Mark Lommel,¹ Michel Bagnat,² and Sabine Strahl^{1*}

Institute of Cell Biology and Plant Physiology, University of Regensburg, 93040 Regensburg,¹ and Max Planck Institute of Molecular Cell Biology and Genetics, 01307 Dresden,² Germany

Received 4 June 2003/Returned for modification 28 July 2003/Accepted 25 September 2003

Protein O mannosylation is a crucial protein modification in uni- and multicellular eukaryotes. In humans, a lack of O-mannosyl glycans causes congenital muscular dystrophies that are associated with brain abnormalities. In yeast, protein O mannosylation is vital; however, it is not known why impaired O mannosylation results in cell death. To address this question, we analyzed the conditionally lethal *Saccharomyces cerevisiae* protein O-mannosyltransferase *pmt2 pmt4Δ* mutant. We found that *pmt2 pmt4Δ* cells lyse as small-budded cells in the absence of osmotic stabilization and that treatment with mating pheromone causes pheromone-induced cell death. These phenotypes are partially suppressed by overexpression of upstream elements of the protein kinase C (PKC1) cell integrity pathway, suggesting that the PKC1 pathway is defective in *pmt2 pmt4Δ* mutants. Congruently, induction of Mpk1p/Slt2p tyrosine phosphorylation does not occur in *pmt2 pmt4Δ* mutants during exposure to mating pheromone or elevated temperature. Detailed analyses of the plasma membrane sensors of the PKC1 pathway revealed that Wsc1p, Wsc2p, and Mid2p are aberrantly processed in *pmt* mutants. Our data suggest that in yeast, O mannosylation increases the activity of Wsc1p, Wsc2p, and Mid2p by enhancing their stability. Reduced O mannosylation leads to incorrect proteolytic processing of these proteins, which in turn results in impaired activation of the PKC1 pathway and finally causes cell death in the absence of osmotic stabilization.

Protein O mannosylation is initiated at the endoplasmic reticulum (ER) by the transfer of mannose from dolichyl phosphate-activated mannose to serine or threonine residues of secretory proteins (52). This reaction is catalyzed by an essential family of protein O-mannosyltransferases (PMTs) that is evolutionarily conserved from yeast to humans (28, 52, 57). The PMT family is divided into the PMT1, PMT2, and PMT4 subfamilies, whose members include transferases closely related to *Saccharomyces cerevisiae* Pmt1p, Pmt2p, and Pmt4p, respectively (17, 57). In *S. cerevisiae* the entire PMT family is highly redundant (Pmt1 to Pmt7p), and members of the PMT1 and PMT2 subfamilies show marked similarities and distinctions from PMT4 subfamily members. For example, members of the PMT1 subfamily (Pmt1p and Pmt5p) interact in pairs with members of the PMT2 subfamily (Pmt2p and Pmt3p), whereas the unique representative of the PMT4 subfamily forms homomeric complexes (16). Further, the PMT1/PMT2 and PMT4 subfamilies use different acceptor protein substrates in vivo (10, 14).

Studies of *pmt* mutants revealed that protein O mannosylation plays a substantial role in uni- and multicellular eukaryotes. In humans, mutations in *POMT1* (protein O-mannosyltransferase 1 gene), which encodes a putative counterpart of the yeast Pmt4p O-mannosyltransferase, result in Walker-Warburg syndrome, which is characterized by severe congenital

muscular dystrophy, a neuronal migration defect, and structural abnormalities of the eye (2). Mutations of the *Drosophila* *POMT1* orthologue *rotated abdomen* alter muscle structures and the alignment of the adult cuticle (38). In *S. cerevisiae*, the simultaneous knockout of particular combinations of three PMT family members (*PMT1*, *PMT2*, and *PMT4* or *PMT2*, *PMT3*, and *PMT4*) is lethal (13). Other *S. cerevisiae* *pmt* mutants, such as *pmt2 pmt4Δ* mutants, are nonviable in the absence of osmotic stabilization and at elevated temperatures (13). In addition, *pmt2 pmt4Δ* cells form large clumps during vegetative growth and show increased sensitivity to Calcofluor white and caffeine. These phenotypes resemble those of yeast mutants with defects in the assembly, organization, or maintenance of a rigid cell wall (22, 31), leading to the conclusion that O-linked glycans are indispensable for cell wall structure and stability (13). However, exactly how O mannosylation contributes to cell wall integrity in yeast is unknown.

During vegetative growth, periods of environmental stress, and pheromone-induced morphogenesis, the integrity of the yeast cell wall is controlled by the protein kinase C (PKC1) cell integrity pathway (22). Alterations of the cell wall of *S. cerevisiae* are sensed by plasma membrane proteins of the WSC family (Wsc1 to Wsc4p) (19, 55) and by Mid2p and its homologue Mtl1p (30, 46). For Wsc1p and Mid2p, it was shown that upon activation, they stimulate the exchange activity of the guanine nucleotide exchange factor Rom2p and thereby activate the small GTPase Rho1p (3, 8, 44), which in turn activates the protein kinase C Pkc1p (42). Pkc1p turns on a mitogen-activated protein (MAP) kinase cascade that consists of a MAP kinase kinase kinase (Bck1p/Slk1p) (6, 34), a pair of

* Corresponding author. Mailing address: Lehrstuhl für Zellbiologie und Pflanzenphysiologie, Universität Regensburg, 93040 Regensburg, Germany. Phone: 49-(0)941-943-3024. Fax: 49-(0)941-943-3352. E-mail: sabine.strahl@biologie.uni-regensburg.de.

TABLE 1. Yeast strains

Strain	Genotype	Reference
SEY6210	<i>MAT</i> α <i>his3</i> - Δ 200 <i>leu2</i> -3-112 <i>lys2</i> -801 <i>trp1</i> - Δ 901 <i>ura3</i> -52 <i>suc2</i> - Δ 9	47
SEY6211	<i>MAT</i> α <i>his3</i> - Δ 200 <i>leu2</i> -3-112 <i>ade2</i> -101 <i>trp1</i> - Δ 901 <i>ura3</i> -52 <i>suc2</i> - Δ 9	47
XMA0-2L	SEY6210 except <i>pmt2</i> Δ :: <i>LEU2</i>	37
XMA1-2L	SEY6211 except <i>pmt2</i> Δ :: <i>LEU2</i>	14
XMA0-4T	SEY6210 except <i>pmt4</i> :: <i>TRP1</i>	24
XMA1-4T	SEY6211 except <i>pmt4</i> :: <i>TRP1</i>	14
<i>pmt2 pmt4</i> mutant	<i>MAT</i> α <i>his3</i> - Δ 200 <i>leu2</i> -3-112 <i>lys2</i> -801 <i>trp1</i> - Δ 901 <i>ura3</i> -52 <i>suc2</i> - Δ 9 <i>pmt2</i> Δ :: <i>LEU2</i> <i>pmt4</i> :: <i>TRP1</i>	13

redundant MAP kinases (Mkk1p and Mkk2p) (25), and a MAP kinase (Mpk1/Slk2) (33, 40). Signaling through the PKC1 MAP kinase cascade leads to a number of cellular responses, one of which is the transcriptional activation of a variety of genes that have been implicated in cell wall assembly and structure (22).

The WSC family in *S. cerevisiae* has four members, encoded by the *WSC1/HCS77/SLG1*, *WSC2*, *WSC3*, and *WSC4* genes (19, 26, 55). These proteins are required for the viability of yeast cells during vegetative growth under various stress conditions, including heat stress and treatment with hydrogen peroxide, ethanol, or DNA-damaging drugs (19, 55, 59). Among the WSC family members, Wsc1p plays the major role in maintaining cell wall integrity. *wsc1* Δ mutants display a cell lysis defect at 37°C (19, 55). Deletion of *WSC2* and *WSC3* does not cause obvious cell lysis but exacerbates the defect when combined with *wsc1* Δ (46, 55). The cell lysis phenotype of *wsc* Δ mutants is caused by cell wall weakening due to an inability to activate the PKC1 pathway (55); it is suppressed by osmotic stabilizers or by overexpression of other WSC family members and components of the PKC1 pathway, such as *PKC1* (19, 55). Deletion of *WSC4* does not exaggerate the cell lysis defect of *wsc1* Δ mutants but increases their sensitivity to ethanol and DNA-damaging drugs (59).

Mid2p is required for the growth of yeast primarily during pheromone-induced morphogenesis (30, 43, 46). Upon treatment with mating pheromone, *mid2* Δ mutants fail to activate the PKC1 pathway at the onset of morphogenesis and consequently die (30, 46). Overexpression of *WSC1* partially rescues the pheromone-induced cell death of *mid2* Δ mutants (46). In addition, the simultaneous deletion of *MID2* and *WSC1* results in a severe osmotic-remedial cell lysis defect during vegetative growth at room temperature (30, 46), indicating that *WSC1* and *MID2* fulfill partially overlapping functions.

The WSC family members and Mid2p are type I transmembrane proteins with similar overall structures that in the case of Wsc1p and Mid2p reside in the plasma membrane (30, 36, 46, 55). These proteins have small cytoplasmic and large extracellular protein domains; the latter contain numerous serine and threonine residues. These Ser-Thr-rich regions are highly O-mannosylated and are important for Wsc1p and Mid2p activity in vivo (30, 36, 44). Mid2p is glycosylated by the mannosyltransferase Pmt2p, and Pmt2p-dependent O-mannosylation is required for wild-type Mid2p function (44).

To elucidate how impaired O-mannosylation affects cell wall integrity and ultimately results in cell death, we analyzed the conditionally lethal *S. cerevisiae pmt2 pmt4* Δ mutant. We present evidence that *pmt2 pmt4* Δ mutants fail to activate the PKC1 cell integrity pathway during mating and in response to external stresses, due to incomplete O-mannosylation of the

plasma membrane sensors Wsc1p, Wsc2p, and Mid2p. In addition, we show that a lack of O-mannosyl glycans causes un-specific processing of those sensor proteins, suggesting that reduced O-mannosylation results in unspecific cleavage of the PKC1 pathway sensor proteins, which in turn results in impaired activation of the cell integrity pathway in response to cell wall stress.

MATERIALS AND METHODS

Yeast strains and plasmids. The *S. cerevisiae* strains used in this study are listed in Table 1. Yeast strains were grown on YPD or SC dropout medium (29) without or supplemented with 1 M sorbitol at 30°C. Yeasts were transformed by the method of Gietz et al. (15) with the yeast shuttle vectors pRS423 (5), pRS416 (5), YEp352 (23), pSB53 (53), YEp352-PMT2 (37), YEp352-PKC1 (56), YEp352-HCS77-HA (46), and YEp352-MID2-HA (46) and the plasmids listed below.

Standard procedures were used for all DNA manipulations (50). All cloning and transformations were carried out in the *Escherichia coli* host SURE2 (Stratagene). Oligonucleotide sequences are available upon request. PCR fragments were routinely checked by sequence analysis.

(i) **Plasmid pRS416-WSCIHA (*CEN WSC1*^{HA}).** A 2.1-kb *KpnI*-*SalI* fragment was isolated from plasmid YEp352-HCS77-HA and cloned into pRS416 (cut with *KpnI* and *SalI*).

(ii) **Plasmid pML1 (*CEN WSC2*^{HA}).** A 1.1-kb *EcoRI*-*SacI* fragment (isolated from plasmid pREP3x-adh, a gift of T. Willer) that contains three copies of the hemagglutinin (HA) sequence and the *Schizosaccharomyces pombe nmt1* transcriptional terminator (39) was cloned into the multiple cloning site of vector pRS416, resulting in plasmid pRS416HA. To create an HA-tagged version of *WSC2*, the *WSC2* promoter and coding region (bp -703 to +1508) were amplified by PCR from plasmid pIRIS18 (55) by using oligonucleotides oligo294 and oligo295. The PCR fragment was digested with *EcoRI* and *NotI* and cloned into pRS416HA cut with the same enzymes. In the resulting plasmid (pML1), nucleotides encoding three copies of the HA epitope were fused in frame to nucleotides encoding the C terminus of *WSC2*.

(iii) **Plasmid pRS416-MID2HA (*CEN MID2*^{HA}).** A 2.2-kb *KpnI*-*SalI* fragment was excised from plasmid YEp352-MID2-HA and cloned into pRS416 digested with *KpnI* and *SalI*.

(iv) **Plasmid pML2 (2 μ m *PMT1*).** A 3.3-kb *BamHI* fragment was excised from plasmid pSB53 and cloned into pRS423 digested with the same enzyme.

(v) **Plasmid pRG4 (2 μ m *MID2*^{ProtA}).** To create a protein A-tagged version of Mid2p, the promoter and coding regions (bp -735 to +1128) were amplified by PCR from plasmid pRS416-MID2HA by using oligonucleotides oligo471 and oligo479. The PCR fragment was digested with *PstI* and *BspEI* and cloned into YCplac33ZZ (a gift of J. Stolz) cut with the same enzymes. In the resulting plasmid (pRG2), nucleotides encoding two copies of the protein A sequence were fused in frame to nucleotides encoding the C terminus of *MID2*. From plasmid pRG2, the *MID2*^{ProtA} open reading frame was amplified by PCR with oligonucleotides oligo501 and oligo502. The PCR fragment was digested with *MfeI* and cloned into the *EcoRI* site of plasmid pNEV-E (a gift of J. Stolz).

Analysis of the terminal cell lysis phenotype. The yeast *pmt2 pmt4* Δ mutant strain was grown to a density of 2×10^7 to 4×10^7 cells/ml at 30°C in YPD medium supplemented with 1 M sorbitol (YPDS). Duplicate portions of 2×10^7 cells were harvested and incubated in 1 ml of YPD or YPDS at 30°C with moderate shaking. Viability was measured over time by plating triplicate samples onto YPDS and staining cells with the vital dye methylene blue in 1 M sorbitol as described previously (49). CFU were counted after incubation for 4 days at 30°C.

Pheromone-induced killing. *MATa* strains were grown at 30°C in YPD or in SC medium lacking uracil but supplemented with 1 M sorbitol (SCS) to a density of 2×10^7 to 4×10^7 cells/ml. A total of 2×10^7 cells were harvested and incubated in 1 ml of the same medium at 30°C for 30 min. Cells were then treated with α -factor (15 μ g/ml) (Bachem). Viability was measured over time as described above.

Multicopy suppression of the osmotic stability defect. Cells were grown at 30°C in SCS without uracil to a density of 2×10^7 to 4×10^7 cells/ml. A total of 10^8 cells were harvested and resuspended in 100 μ l of 1 M sorbitol. Serial 10-fold dilutions were prepared in 1 M sorbitol, and 10 μ l of each dilution was spotted onto YPD and YPDS plates, which were then incubated for 3 days at 30°C.

Measurement of Mpk1p phosphotyrosine content upon pheromone treatment and temperature shift. Wild-type SEY6211 and *pmt2 pmt4* Δ mutant strains were grown in SCS to a density of 2×10^7 to 4×10^7 cells/ml at 30°C. A total of 2×10^7 cells were harvested, incubated in 1 ml of SCS at 30°C for 30 min with moderate shaking, and then incubated with α -factor (75 μ g/ml for 3 h) or at high temperature (37°C for 3 h). Cells were collected by centrifugation at $20,000 \times g$ for 1 min at 4°C, resuspended in 50 μ l of $3 \times$ sodium dodecyl sulfate (SDS) sample buffer, and incubated at 95°C for 4 min. Cell debris was pelleted by centrifugation at $20,000 \times g$ for 1 min. Thirty microliters of the supernatant was resolved on SDS-10% polyacrylamide gels.

Preparation of crude membranes. Crude membranes were isolated as described previously (17).

Immunoprecipitation. Mid2p^{HA} was solubilized from crude membranes in 500 μ l of solubilization buffer (50 mM Tris-HCl [pH 7.5], 140 mM NaCl, 1 mM EDTA, 2% Triton X-100, 10% glycerol, 1 mM phenylmethylsulfonyl fluoride, 1 mM benzamide, 0.25 mM TLCK [α -*p*-tosyl-L-lysine chloromethyl ketone], 50 μ g of TPCK [tosylsulfonyl phenylalanyl chloromethyl ketone] per ml, 10 μ g of aprotinin per ml, 1 μ g of leupeptin per ml, and 1 μ g of pepstatin per ml) by vortexing for 30 min at 4°C. The suspension was clarified by centrifugation for 30 min at $48,000 \times g$ to obtain the Triton extract. HA-tagged Mid2p was immunoprecipitated for 1 h at 4°C from 300 μ l of Triton extract by using 10 μ l of anti-HA monoclonal antibodies covalently coupled to protein A-Sepharose (16B12; Babco). Precipitates were washed four times with 1 ml of cold solubilization buffer and once with 1 ml of Tris-buffered saline.

Deglycosylation by Endo H digestion. Immunoprecipitates or 5 μ l of crude membranes were suspended in 25 μ l of endoglycosidase H (Endo H) buffer (50 mM potassium phosphate buffer [pH 5.5] containing 0.02% SDS, 0.1 M 2-mercaptoethanol, and protease inhibitors as described above) and digested with 1 to 5 U of Endo H (Calbiochem) per μ l for 2 h at 37°C. Mock incubations were carried out without Endo H. Reactions were stopped by adding 10 μ l of $5 \times$ SDS sample buffer.

Deglycosylation by α -mannosidase digestion. Immunoprecipitates were resuspended in 20 μ l of mannosidase buffer (0.125 M acetic acid-NaOH [pH 5.0] containing 0.01% bovine serum albumin, 0.1 mM ZnSO₄, and protease inhibitors as described above) and digested with 1 to 5 U of α -1,2,3,6-mannosidase (Calbiochem) per μ l for 2 h at 37°C. Mock incubations were carried out without α -mannosidase. Reactions were stopped by adding 10 μ l of $5 \times$ SDS sample buffer.

Western blot analysis. Proteins were fractionated by SDS-polyacrylamide gel electrophoresis (SDS-PAGE) and transferred to nitrocellulose membranes (20). Polyclonal anti-phospho-p44/p42 MAP kinase antibodies (Cell Signaling Technology) were used at a dilution of 1:1,000, anti-Wbp1p antibodies (54) were used at a dilution of 1:2,000, and anti-Pfk1p antibodies (a gift of J. Heinisch) were used at a dilution of 1:50,000. The anti-HA (16B12; Babco) monoclonal antibodies were used at 1:5,000 dilution. Protein-antibody complexes were visualized by enhanced chemiluminescence with the Amersham ECL system. Different amounts of membrane proteins and exposure times of the X-ray films were tested to ensure detection of qualitative and quantitative differences.

Pulse-chase labeling. Cells were grown to mid-log phase in YPD medium at 24°C to an optical density at 600 nm (OD₆₀₀) of about 1. Cells were collected by centrifugation, washed with SC medium without methionine, and resuspended in fresh medium to a density of 4 OD₆₀₀ units/ml. After 15 min of incubation at 24°C, cells were pulse-labeled with 1.5 mCi of [³⁵S]methionine (New England Nuclear) for 3 min. Cells were chased with excess methionine, and samples of 4 OD₆₀₀ units taken at various times and then incubated on ice with 0.2% sodium azide for 5 min. Cells were washed in water and frozen on dry ice. Frozen cells were resuspended in 0.55 ml of lysis buffer (50 mM Tris-HCl [pH 8.0], 150 mM NaCl, 2 mM EDTA) containing protease inhibitors and lysed by vortexing with glass beads for 5 min at 4°C. Lysates were cleared by centrifugation (3 min, $2,000 \times g$) and incubated with NP-40 (1%) and SDS (0.1%) for 5 min at 37°C. After removal of insoluble material by centrifugation (1 min, $6,000 \times g$), lysates (0.4 ml) were mixed with 1 ml of immunoprecipitation buffer (10 mM Tris-HCl [pH

7.4], 150 mM NaCl, 2 mM EDTA, 1% NP-40, 0.1% SDS) containing protein A-Sepharose (Amersham) and 5 μ l of rabbit anti-HA antiserum (Santa Cruz Biotechnology). After a 3-h incubation at room temperature, immunoprecipitates were washed four times with immunoprecipitation buffer and once with 10 mM Tris-HCl [pH 7.4] and then resuspended in 30 μ l of sample buffer. Samples were analyzed by SDS-PAGE and autoradiography.

Protein purification and sequence analysis of Mid2p^{ProtA}. *pmt2* Δ mutant cells transformed with pRG4 were grown at 30°C in 5 liters of SC medium lacking uracil to a density of 6×10^7 to 7×10^7 cells/ml. Cells were harvested, resuspended in 5 liters of YPD, and grown to a final density of 20×10^7 to 30×10^7 cells/ml. Cells were harvested, washed with 100 ml of water, and resuspended to a total volume of 60 ml in 50 mM Tris-HCl (pH 7.5) containing 1 mM phenylmethylsulfonyl fluoride and 1 mM benzamide. An equal volume of glass beads was added, and cells were lysed in an MSK cell homogenizer for 5 min under CO₂ cooling. Cell debris was removed by centrifugation for 5 min at $4 \times g$ at 4°C. Crude membranes were collected from the supernatant by centrifugation for 30 min at $48,000 \times g$ at 4°C (Sorvall SS34 rotor). The membrane pellet was resuspended in solubilization buffer (20 mM KPi [pH 8.0], 150 mM KCl, 5 mM MgCl₂, and protease inhibitors) to a total volume of 90 ml. To solubilize Mid2p^{ProtA}, Triton X-100 was added to a final concentration of 1%. Solubilization was performed at room temperature for 20 min on an IKA Vibrax VXR shaker. The suspension was clarified by centrifugation for 1 h at $120,000 \times g$ at 4°C (Ti 60 rotor; Beckman). The supernatant was incubated for 1 h at 4°C with 600 μ l of Sepharose CL4B (Amersham) and then overnight at 4°C with 400 μ l of immunoglobulin G (IgG)-Sepharose (IgG-Sepharose 6 Fast Flow; Amersham). The IgG-Sepharose beads were washed three times with 500 μ l of solubilization buffer and three times with 500 μ l of 5 mM ammonium acetate (pH 5.0). Mid2p^{ProtA} was eluted with 500 μ l of 0.5 M acetic acid (pH 3.4). The eluate was neutralized with 175 μ l of 1 M Tris base. Eluted proteins were trichloroacetic acid precipitated, separated on an SDS-10% polyacrylamide gel, blotted onto a polyvinylidene difluoride membrane, and stained with Coomassie brilliant blue R250 (Serva).

Proteins were sequenced with a Procise 492A sequencer (PE Biosystems), with on-line detection of the phenylthiohydantoin amino acids, according to the manufacturer's instructions.

RESULTS

Conditionally lethal *pmt* mutants such as *pmt2 pmt4* Δ mutants are nonviable in the absence of osmotic support (13), suggesting that O mannosylation is important for the synthesis and/or maintenance of an intact cell wall, a vital structure in yeast cells. To address the question of how O mannosylation affects yeast cell wall integrity, we analyzed the *S. cerevisiae pmt2 pmt4* Δ mutant in detail.

***pmt2 pmt4* Δ mutant cells show terminal cell lysis as small-budded cells and mating pheromone-induced cell death.** *pmt2 pmt4* Δ mutant cells are able to grow in the presence of 1 M sorbitol at 30°C. However, in liquid culture, the growth rate is reduced compared to that of the wild-type strain SEY6211 (doubling time of 185 min versus 115 min), and mutant cells form large aggregates (Fig. 1A, right panel). Upon shift to medium without sorbitol, cells cease growth (Fig. 1A; see Fig. 3A). Determination of the number of survivors over time revealed that after a 4-h incubation period, ~80% of the cells were usually dead (data not shown). Microscopic examination showed the accumulation of cells with small buds that stained intensely with the vital dye methylene blue (Fig. 1A, left panel). This observed terminal cell lysis phenotype is characteristic of mutants defective in the PKC1 cell integrity pathway (19, 33, 35). We therefore tested whether *pmt2 pmt4* Δ mutants have other phenotypes typical of mutants defective in the PKC1 pathway, such as mating pheromone-induced cell death (22). Treatment of *MATa pmt2 pmt4* Δ cells with the mating pheromone α -factor in the presence of 1 M sorbitol resulted in >90% cell death after an incubation period of 7 h (Fig. 1B).

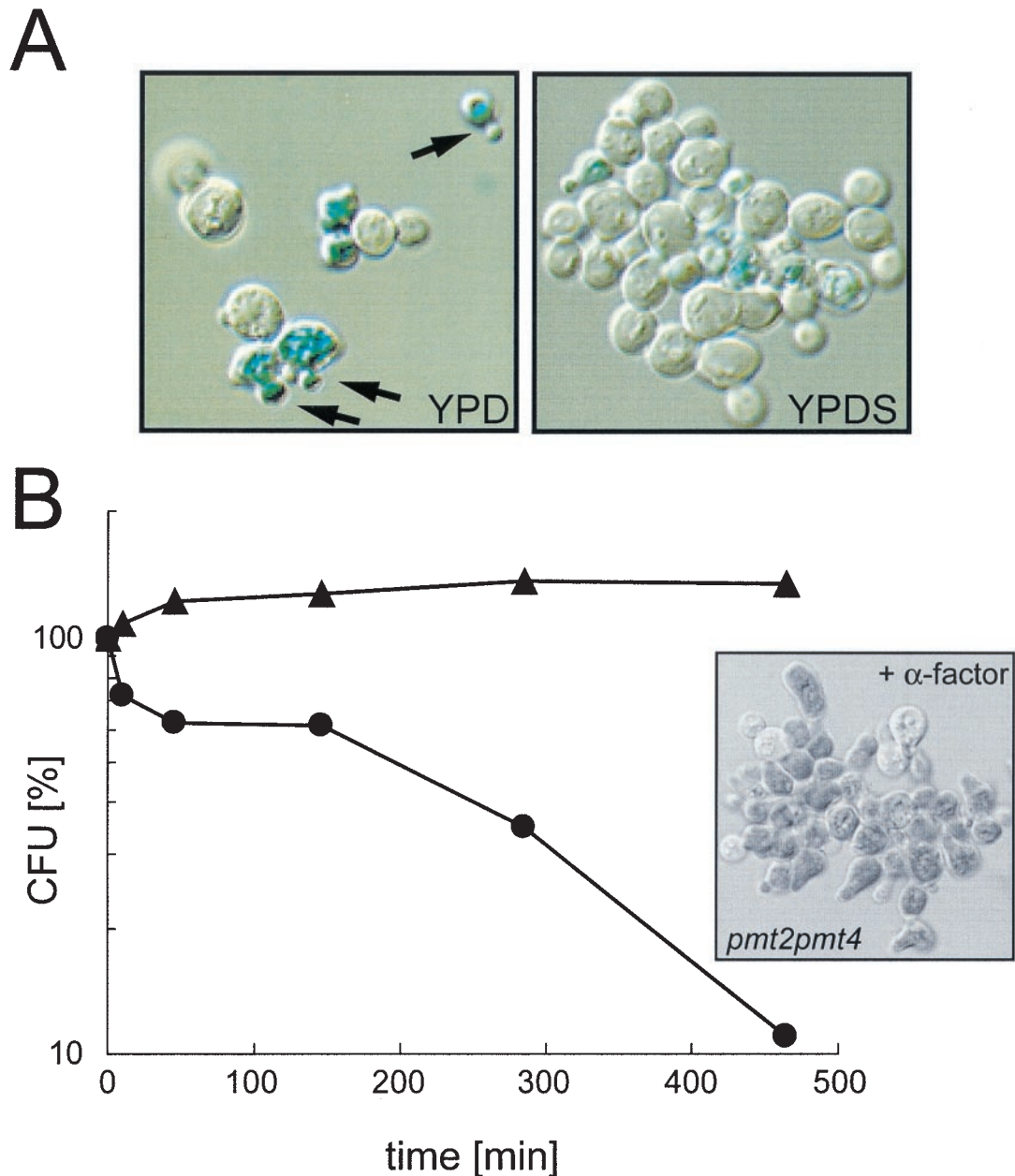


FIG. 1. Terminal cell lysis (A) and mating-induced cell death (B) of the *pmt2 pmt4* Δ mutant. (A) Log-phase cells of the *pmt2 pmt4* Δ strain were grown in YPD liquid medium in the presence (right panel) or absence (left panel) of 1 M sorbitol for 4 h. Cells were stained with the vital dye methylene blue. Arrows indicate dead cells, which appear dark blue. (B) Wild-type strain SEY6211 (▲) and the *pmt2 pmt4* Δ mutant (●) were grown in YPDS at 30°C and treated with α -factor as described in Materials and Methods. At the indicated times, viability was measured by plating onto YPDS. CFU were counted after 4 days at 30°C. Average values from two independent experiments are shown. The inset shows *pmt2 pmt4* Δ cells stained with methylene blue after 4.75 h of α -factor treatment.

Methylene blue staining revealed that cells arrested and died at the onset of morphogenesis when the mating projection is formed (Fig. 1B). This phenotypic characterization indicates that the *pmt2 pmt4* Δ mutant resembles mutants with defects in the cell integrity pathway, such as *pkc1* Δ (35) or *mid2* Δ *wsc1* Δ (30, 46) mutants.

Impaired phosphorylation of Mpk1p in response to mating pheromone or heat stress. To explore further whether the cell integrity pathway is affected in *pmt2 pmt4* Δ mutants, we ana-

lyzed the activation of the PKC1 pathway by measuring the activity of the MAP kinase Mpk1p/Slt2p. During pheromone induction or temperature stress, Mpk1p activity increases as a result of tyrosine phosphorylation of the protein (4, 58). Therefore, we measured Mpk1p phosphorylation in wild-type and *pmt2 pmt4* Δ mutant strains after pheromone treatment by using a phospho-specific p44/42 MAP kinase antibody. As shown in Fig. 2, *pmt2 pmt4* Δ mutants do not show increased Mpk1p phosphorylation in response to the mating pheromone α -factor

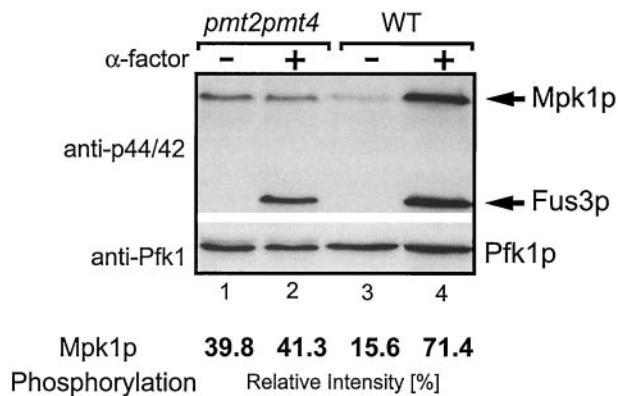


FIG. 2. Mpk1p phosphorylation in response to α -factor is impaired in the *pmt2 pmt4* mutant. The *pmt2 pmt4* mutant (lanes 1 and 2) and wild-type (WT) strain SEY6211 (lanes 3 and 4) were treated with α -factor for 3 h or mock treated as indicated. Cell extracts were prepared as described in Materials and Methods. Proteins were resolved on SDS-10% polyacrylamide gels and analyzed by Western blotting. Blots were sequentially probed with polyclonal anti-phospho-p44/p42 MAP kinase antibodies (upper panel) and polyclonal anti-Pfk1p antibodies (lower panel). Arrows indicate the MAP kinases Mpk1p and Fus3p. Pfk1p indicates equal loading of the lanes. Western signals were quantified by using Optiquant (Packard BioScience) software. Band intensities of phospho-Mpk1p were normalized according to the relative intensities of Pfk1p to correct loading variations of the polyacrylamide gels. Average values from three independent experiments are shown.

(lanes 1 and 2). Quantification of phospho-Mpk1p revealed that in wild-type yeast, Mpk1p phosphorylation increases up to 4.6-fold after α -factor treatment (Fig. 2, lanes 3 and 4), but no such increase is seen in the *pmt2 pmt4* mutant (Fig. 2, lanes 1 and 2). Interestingly, under noninduced conditions in *pmt2 pmt4* cells, the level of phospho-Mpk1p was approximately 2.5-fold higher than that in wild-type cells (Fig. 2, compare lanes 1 and 3). Although the difference was small, it was highly reproducible. In contrast, phosphorylation of the MAP kinase Fus3p (1, 11), which is activated in response to α -factor by a pheromone-induced MAP kinase cascade, increased at the same rate in both strains (Fig. 2, lanes 2 and 4). This indicates that *pmt2 pmt4* mutants specifically fail to activate the PKC1 pathway. Similar results were obtained upon mild heat treatment (37°C) (data not shown). From these data, we conclude that the PMTs are required for efficient signaling in the PKC1 pathway.

Overexpression of *PKC1*, *WSC1*, or *MID2* suppresses the cell lysis defect and mating pheromone sensitivity of *pmt2 pmt4* mutants. The plasma membrane sensors of the PKC1 pathway, Mid2p and Wsc1p, are O mannosylated (30, 36, 46), and therefore it seemed likely that their modification is affected in *pmt2 pmt4* mutants. Because overexpression of *PKC1* suppresses the cell lysis defect of a *mid2* Δ *wsc1* Δ mutant (30), we investigated whether this also applies to *pmt2 pmt4* mutants. We found that expression of high-copy *PKC1* to some extent suppresses both the cell lysis defect in nonosmotically stabilized medium at 30°C (Fig. 3A) and the pheromone-induced cell death (Fig. 3B). Interestingly, overexpression of *MID2* or *WSC1* also partly restores the growth of *pmt2 pmt4* cells in the absence of 1 M sorbitol (Fig. 3A). In addition, multicopy

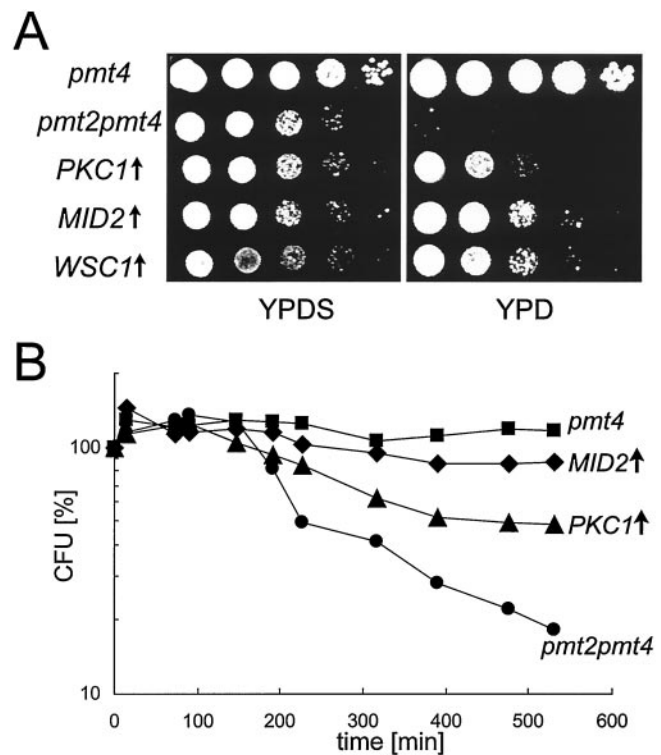


FIG. 3. Overexpression of members of the PKC1 pathway suppresses *pmt2 pmt4* conditional lethal phenotypes. The *pmt2 pmt4* mutant was transformed with YEp352-PMT2 (*pmt4*, ■), YEp325 (*pmt2 pmt4*, ●), YEp352-*PKC1* (*PKC1* ↑, ▲), YEp352-*MID2*-HA (*MID2* ↑, ◆), and YEp352-*HCS77*-HA (*WSC1* ↑) and grown in SCS without uracil to exponential phase. (A) *PKC1*, *MID2*, and *WSC1* partially suppress the cell lysis phenotype. A total of 10^5 cells of the strains indicated and 10-fold serial dilutions thereof were spotted onto YPD and YPDS plates and incubated for 3 days at 30°C. (B) *PKC1* and *MID2* suppress the pheromone-induced cell death. Cells were treated with α -factor in SCS without uracil, and viability was measured at the indicated times as described in Materials and Methods. Average values from two independent experiments are shown.

expression of *MID2* rescues *pmt2 pmt4* cells from pheromone-induced cell death. As shown in Fig. 3B, 88% of *pmt2 pmt4* cells overexpressing *MID2* survived a treatment with α -factor for 8.8 h, compared to 18% of *pmt2 pmt4* cells transformed with a control plasmid. Expression of *PKC1*, *MID2*, or *WSC1* from single-copy plasmids failed to suppress the growth defects of *pmt2 pmt4* cells (data not shown).

Our data so far suggested that signaling of cell wall stress through the PKC1 pathway is impaired in *pmt2 pmt4* mutants. Because the phenotypes of *pmt2 pmt4* mutants closely resemble those of *mid2* Δ *wsc1* Δ mutants (30, 44), we analyzed the effect of protein O mannosylation on Wsc1p, Wsc2p, and Mid2p, upstream activators of the PKC1 pathway.

O mannosylation of Wsc1p and Wsc2p is impaired in *pmt* mutants. To investigate the WSC family members biochemically, we expressed single-copy, C-terminally HA epitope-tagged versions of Wsc1p and Wsc2p in wild-type yeast and the *pmt2 pmt4* mutant. Crude membranes were prepared, and Wsc proteins were analyzed with SDS-8% polyacrylamide gels and Western blotting, using monoclonal anti-HA antibodies. Wsc1p^{HA} and Wsc2p^{HA} have deduced molecular masses of

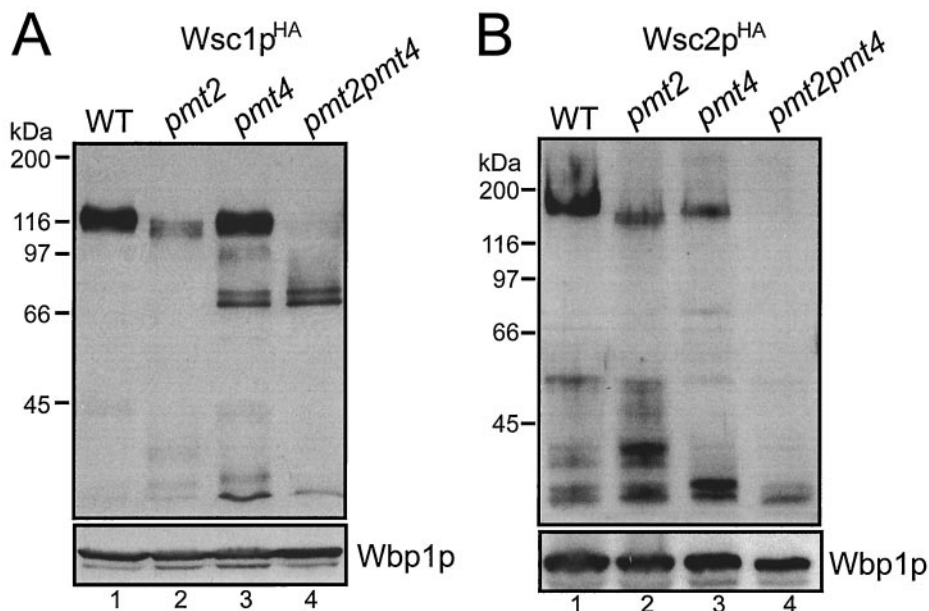


FIG. 4. Impaired O mannosylation and stability of Wsc1p and Wsc2p in *pmt* mutants. Western blots of crude membranes (30 μ g of protein) isolated from yeast strain SEY6210 (wild type [WT]) (lane 1) and the *pmt2* Δ (lane 2) (XMA0-2L), *pmt4* Δ (lane 3) (XMA0-4T), and *pmt2 pmt4* Δ (lane 4) mutants expressing single-copy plasmid pRS416-WSC1HA (Wsc1p^{HA}) (A) or pML1 (Wsc2p^{HA}) (B) are shown. Proteins were resolved on SDS-8% polyacrylamide gels. Blots were sequentially probed with monoclonal anti-HA and polyclonal anti-Wbp1p antibodies. Wbp1p indicates equal loading of the lanes.

42.8 and 55.8 kDa, respectively. The mature Wsc1p^{HA} and Wsc2p^{HA} proteins isolated from wild-type yeast show apparent molecular masses of ~110 to 120 kDa and ~160 to 200 kDa, respectively, due to a high number of O-linked polymannose chains (Fig. 4, lanes 1) (36, 46). Both proteins contain N-glycosylation sequons but are not N glycosylated in vivo (reference 46 and data not shown). Strikingly, in *pmt2 pmt4* Δ mutants Wsc1p^{HA} and Wsc2p^{HA} were not detected as bands of the expected molecular masses (Fig. 4, lanes 4). In the case of Wsc1p^{HA}, a faint smear of ~100 to 68 kDa, two distinct bands of 71 and 68 kDa, and fragments smaller than 35 kDa were specifically detected by the anti-HA antibodies (Fig. 4A, lane 4); in the case of Wsc2p^{HA}, only protein fragments with molecular masses of less than 35 kDa were recognized (Fig. 4B, lane 4). These data suggested that Wsc1p^{HA} and Wsc2p^{HA} are O mannosylated by either Pmt2p, Pmt4p, or both and that a lack of O mannosylation affects the stability of the proteins. In order to test whether Pmt2p or Pmt4p individually affects the maturation of the Wsc proteins, we analyzed Wsc1p^{HA} and Wsc2p^{HA} in *pmt2* Δ and *pmt4* Δ single mutants. As shown in Fig. 4A, in the absence of Pmt2p the molecular mass of Wsc1p^{HA} slightly decreases, and, even more strikingly, the total amount of the high-molecular-mass form is dramatically reduced, and fragments smaller than 45 kDa are detectable (compare lanes 1 and 2). In the *pmt4* Δ mutant, in addition to an almost normal amount of the mature form of Wsc1p^{HA}, two bands at 71 and 68 kDa and smaller fragments appear (Fig. 4A, lane 3). Similar results were obtained for Wsc2p^{HA}. In the *pmt2* Δ mutant, but not in the *pmt4* Δ strain, the high-molecular-mass form of Wsc2p^{HA} is slightly smaller than that in wild-type cells. In both mutants, however, the total amount of these forms is decreased and fragments of <45 kDa in *pmt2* Δ cells and of <35 kDa in *pmt4* Δ cells arise (Fig. 4B, lanes 2 and 3).

Other membrane proteins, such as Wbp1p (54), a subunit of the oligosaccharyltransferase complex, are not affected in O-mannosylation mutants (Fig. 4, lower panels).

The results indicate that Wsc1p and Wsc2p are substrates of the PMTs Pmt2p and Pmt4p and that diminished O mannosylation affects the stability of the Wsc proteins. Our data further suggest that Pmt2p and Pmt4p differently affect the maturation of Wsc proteins and, therefore, that their simultaneous deletion in *pmt2 pmt4* Δ cells has additive effects.

Overexpression of Pmt1p in *pmt2 pmt4* Δ cells rescues the cell lysis defect and restores Wscp O mannosylation. Pmt1p and Pmt2p form a heteromeric complex and mannosylate a very similar set of protein substrates in vivo (14, 17). Overexpression of *PMT1*, but not of *PMT3*, *PMT5*, or *PMT6*, suppresses the cell lysis phenotype of *pmt2 pmt4* Δ cells (Fig. 5A and data not shown). If cell lysis in the absence of an osmotic stabilizer is primarily due to the maturation defect of the Wsc proteins, one would expect that overexpression of *PMT1* would restore O mannosylation and thereby the stability of Wsc proteins. This is exactly what we observed. Overexpression of *PMT1* compensates for the lack of *PMT2* and almost completely restores the ability of *pmt2 pmt4* Δ cells to produce mature Wsc1p^{HA} in (Fig. 5B). Similar results were obtained for Wsc2p^{HA} (data not shown).

Impaired O mannosylation affects stability of Mid2p. It was previously suggested that Mid2p is O mannosylated exclusively by Pmt2p (44). However, compared to *pmt2 pmt4* Δ strains, *pmt2* Δ mutants show a very mild pheromone-induced cell death phenotype (44). We therefore investigated whether Mid2p is affected differently in *pmt2* Δ mutants than it is in *pmt2 pmt4* Δ mutants. We expressed a single copy of C-terminally HA epitope-tagged Mid2p (see Fig. 7A) in wild-type yeast and *pmt* mutants. Crude membranes were prepared, and

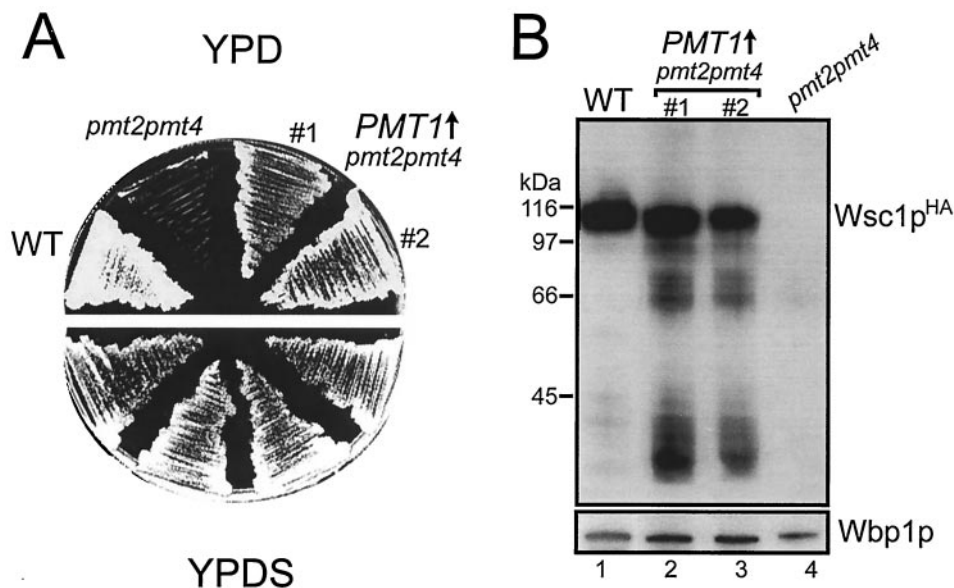


FIG. 5. Overexpression of *PMT1* in the *pmt2 pmt4*Δ mutant. Wild-type (WT) strain SEY6210 was transformed with pRS423, and the *pmt2 pmt4*Δ mutant was transformed with pRS423 (*pmt2 pmt4*) or pML2 (*pmt2 pmt4 PMT1* ↑) (#1 and #2 indicate individual transformants). (A) Strains were grown on SCS plates without histidine for 2 days, restreaked on YPD (upper panel) and YPDS (lower panel) plates, and incubated at 30°C for 4 days. (B) The indicated strains were transformed with single-copy plasmid pRS416-WSC1HA (Wsc1p^{HA}) and grown on SCS without histidine and uracil. Crude membranes (30 μg of protein) were prepared and resolved on SDS–8% polyacrylamide gels. Western blotting was performed by sequential probing with monoclonal anti-HA (upper panel) and polyclonal anti-Wbp1p (lower panel) antibodies.

proteins were analyzed as described above. Mid2p^{HA} has a deduced molecular mass of 40.4 kDa. In wild-type yeast, Mid2p^{HA} shows an apparent molecular mass of >200 kDa. In addition, two smaller protein bands with apparent molecular masses of ~47 and ~40 kDa are specifically detected by the anti-HA antibodies (Fig. 6A, lane 1) (44, 46). In *pmt2 pmt4*Δ cells the >200- and 47-kDa forms of Mid2p^{HA} are absent, whereas the amount of the 40-kDa protein significantly increases (Fig. 6, lanes 4). In addition, a small amount of a ~66-kDa band appears that is not detected in wild-type cells (Fig. 6A, lane 4). A similar pattern is observed in a *pmt4*Δ single mutant, although the ~66-kDa band is detectable only when Mid2p^{HA} is expressed from a 2 μm plasmid (Fig. 6A, lane 7). The pattern changes in a *pmt2*Δ single mutant; only the 40- and 47-kDa variants of Mid2p^{HA} are detected, with the latter being the most abundant protein (Fig. 6, lanes 2). Interestingly, when *MID2*^{HA} was overexpressed from a 2 μm plasmid, in addition to the Mid2p^{HA} variants described, small amounts of Mid2p^{HA} with molecular masses of ~80 to 200 kDa could be detected in *pmt* mutants (Fig. 6A, lanes 6 to 8). From these data we conclude that (i) Pmt2p and Pmt4p differentially affect the maturation of Mid2p and (ii) additional mannosyltransferases are involved in the modification of Mid2p.

To gain further insight into the nature of the different Mid2p variants, we analyzed the glycosylation state of Mid2p^{HA} in more detail. In addition to many O-mannosylation sites, Mid2p has two potential N-glycosylation sites (N \overline{X} S/T) at positions Asn-35 and Asn-211 (Fig. 7A). However, it is not known whether Mid2p is N glycosylated in vivo. Mid2p^{HA} was overexpressed in wild-type, *pmt2*Δ, and *pmt4*Δ strains and purified by immunoprecipitation. Removal of N-linked carbohydrate chains by treatment with Endo H reduced the molecular mass

of mature Mid2p^{HA} isolated from wild-type yeast from >200 to ~150 kDa, demonstrating that Mid2p is N glycosylated in vivo (Fig. 7B, lanes 1 and 2). Eliminating the N-glycosylation site N35SS by site-directed mutagenesis abolished N glycosylation (data not shown), proving that Mid2p is modified by one N-linked carbohydrate chain at position Asn-35. In the *pmt4*Δ mutant, mature Mid2p^{HA} and the ~66-kDa variant are also N glycosylated (Fig. 7B, lanes 5 and 6), but neither the 47-kDa nor the 40-kDa form is modified by N glycosylation (Fig. 7B). These data suggested that decreased O mannosylation either affects N glycosylation of Mid2p or results in at least partial clipping of the N-terminal domain.

To distinguish between these possibilities, pulse-chase labeling experiments were performed. Wild-type, *pmt2*Δ, and *pmt4*Δ cells expressing single-copy *MID2*^{HA} were metabolically pulse-labeled with [³⁵S]methionine for 3 min. After different chase periods, Mid2p^{HA} was immunoprecipitated from whole-cell extracts and analyzed by SDS-PAGE and autoradiography. In wild-type yeast after a labeling period of 3 min, a ~100-kDa Mid2p^{HA} precursor and mature Mid2p^{HA} (>200 kDa) could be detected (Fig. 7C, lane 1). Analysis of Mid2p^{HA} in a *sec18* mutant, which accumulates secretory proteins in the ER at restrictive temperature (18), confirmed that the ~100-kDa protein represents the ER form of Mid2p^{HA} (data not shown). After a chase period of 5 min, the precursor was no longer detected, and the amount of the mature protein increased and did not change further over 15 min (Fig. 7C, lanes 2 and 3). The situation was similar in the *pmt4*Δ mutant. However, in addition to mature Mid2p^{HA}, the 40-kDa form appeared after a 5-min chase period (Fig. 7C, lanes 7 to 9). In contrast, in the *pmt2*Δ mutant, precursor forms with molecular masses of between ~85 and ~75 kDa were detected after the 3-min pulse,

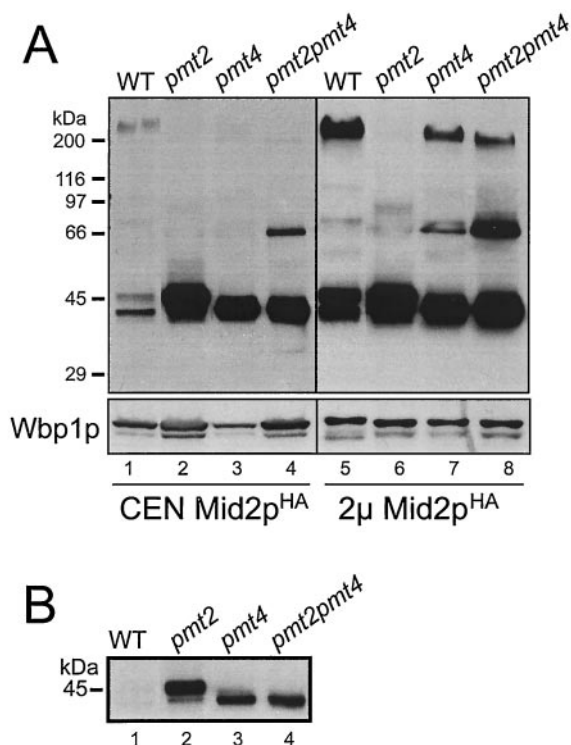


FIG. 6. Impaired O mannosylation of Mid2p in *pmt* mutants. Western blots of crude membranes isolated from the yeast strain SEY6210 (wild type [WT]) and the *pmt2Δ* (XMA0-2L), *pmt4Δ* (XMA0-4T), and *pmt2 pmt4Δ* mutants expressing single-copy plasmid pRS416-MID2HA (CEN Mid2p^{HA}) (lanes 1 to 4) or multicopy plasmid YEp352-MID2-HA (2μ Mid2p^{HA}) (lanes 5 to 8) are shown. Proteins were resolved on SDS–8% polyacrylamide gels. Blots were sequentially probed with monoclonal anti-HA and polyclonal anti-Wbp1p antibodies. The same samples were loaded in each panel; to increase resolution, 30 μg of proteins was loaded in panel A and only 5 μg of protein was loaded in panel B.

indicating that this Mid2p^{HA} variant is heterogeneously glycosylated (Fig. 7C, lane 4). Similar forms of Mid2p^{HA} accumulated in a *sec18 pmt2Δ* mutant after a shift to the restrictive temperature (data not shown), indicating that a less glycosylated ER precursor of Mid2p^{HA} is made in the absence of Pmt2p. In addition, a high-molecular-mass form of Mid2p^{HA} is present (Fig. 7C, lane 4). Strikingly, after a 5-min chase period, the 47-kDa variant appears, and, with time, high-molecular-mass forms of Mid2p^{HA} disappear whereas the 47-kDa form accumulates (Fig. 7C, lanes 5 and 6).

These data indicated that Mid2p is proteolytically processed in *pmt* mutants. To prove these results, we determined the peptide sequence of the N terminus of the 47- and 40-kDa variants of Mid2p. A protein A tag was fused to the carboxyl terminus of Mid2p, and the tagged protein was expressed in a *pmt2Δ* mutant. By using IgG affinity chromatography, the low-molecular-mass variants of Mid2p^{ProtA} were purified, and the N-terminal protein sequences were determined by Edman degradation (for details, see Materials and Methods). For both Mid2p variants, the N-terminal peptide sequence identified is Ala-Asp-Ser-Ser-Asn-Lys-Ser-Lys-Ser and matches amino acids Ala-207 to Ser-215 of mature Mid2p (Fig. 8A). This region is located in the extracellular domain of Mid2p, in close prox-

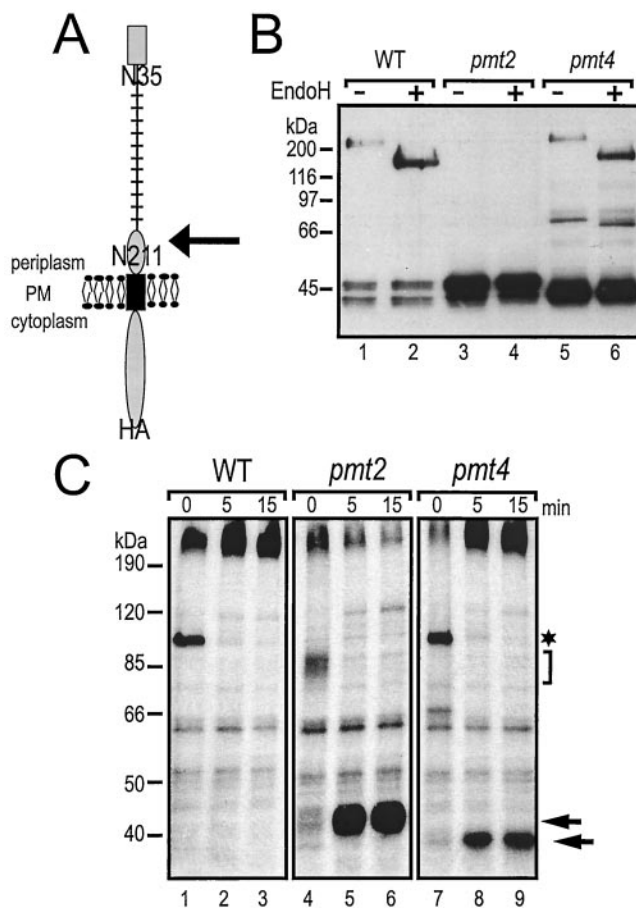


FIG. 7. Processing of Mid2p in *pmt* mutants. (A) Schematic representation of Mid2p^{HA}. Mid2p is a type I membrane protein of the plasma membrane (PM). The C terminus is facing the cytoplasm, and the N terminus is facing the periplasmic space. Black rectangle, transmembrane domain; grey rectangle, signal peptide; stalk structure, O-glycosylated Ser/Thr-rich domain. N35 and N211 indicate putative N-glycosylation sites, but only N35 is glycosylated in vivo. The arrow indicates the site of proteolytic cleavage. (B) Mid2p^{HA} (YEp352-MID2-HA) was expressed in strain SEY6210 (wild type [WT]) and the *pmt2Δ* (XMA0-2L) and *pmt4Δ* (XMA0-4T) mutants and immunoprecipitated with monoclonal anti-HA antibodies coupled to protein A-Sepharose. To remove N-linked carbohydrate chains, the immunoprecipitates were treated with Endo H. Mid2p^{HA} was analyzed by SDS-PAGE and Western blotting with monoclonal anti-HA antibodies. (C) Strain SEY6210 and the *pmt2Δ* (XMA0-2L) and *pmt4Δ* (XMA0-4T) mutants expressing a single copy of MID2^{HA} (pRS416-MID2HA) were pulse-labeled with [³⁵S]methionine as described in Materials and Methods. Samples were separated on 6 to 12% polyacrylamide gels. Autoradiography was performed for 5 days. The asterisk and bracket indicate ER forms of Mid2p^{HA}; arrows indicate the 47- and 40-kDa protein variants.

imity to the putative transmembrane domain (Asn-221 to Cys-249) (Fig. 8A). Interestingly, the signal intensity of all serine residues determined by Edman degradation was low in comparison to that of the other amino acids, suggesting that the serines are partially O mannosylated. Thus, we determined whether the 47- and 40-kDa Mid2p variants are still modified by O-linked polymannose chains. Complete deglycosylation was achieved with α-mannosidase. Deglycosylation of Mid2p^{HA} isolated from both a *pmt2Δ* mutant (Fig. 8B, lanes 1 and 2) and

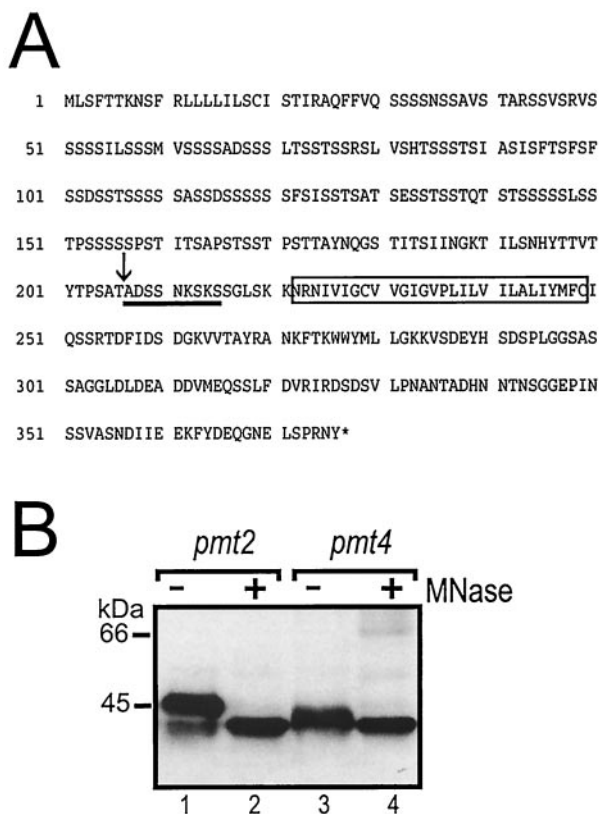


FIG. 8. N-terminal peptide sequence and O mannosylation of the low-molecular-mass Mid2p protein variants. (A) Deduced amino acid sequence of Mid2p. The rectangle marks the putative transmembrane domain. The N-terminal peptide sequence of the 47- and 40-kDa protein variants, obtained by Edman degradation, is underlined. The arrow indicates the cleavage site. (B) Mid2p^{HA} (YE_p352-MID2-HA) was expressed in the *pmt2*Δ (XMA0-2L) and *pmt4*Δ (XMA0-4T) strains and immunoprecipitated with monoclonal anti-HA antibodies coupled to protein A-Sepharose. Complete deglycosylation was achieved by using α-mannosidase (MNase) as described in Materials and Methods. Mid2p^{HA} was analyzed by SDS-PAGE and Western blotting with monoclonal anti-HA antibodies.

a *pmt4*Δ mutant (Fig. 8B, lanes 3 and 4) resulted in a decrease of the apparent molecular masses from 47 and 40 kDa, respectively, to approximately 38 kDa. The same apparent molecular mass was observed for a truncated version of Mid2p^{HA} (deletion of N-terminal amino acids 2 to 206), which was expressed in *E. coli* (data not shown). Taken together, these data show that the low-molecular-mass Mid2p proteins represent truncated forms, with various degrees of O mannosylation.

In summary, our data demonstrate that in the absence of Pmtps, Mid2p is incorrectly processed on its way to or at the plasma membrane.

DISCUSSION

In this study we show that the diminished cell wall integrity of PMT mutants is predominantly a consequence of a loss of activation of the PKC1 pathway during morphogenesis and in response to cell wall stress. Our data suggest that activation fails due to impaired signaling through the plasma membrane sensors of the WSC family and Mid2p, whose stabilities are greatly reduced in *pmt* mutants.

Protein O mannosylation enhances the stability of the WSC family members and Mid2p. Wsc proteins and Mid2p contain serine- and threonine-rich domains that are typical of highly O-mannosylated proteins (30, 46, 55) and that are crucial for protein function, as demonstrated for Wsc1p and Mid2p (36, 44, 46). It was suggested that the modification of those regions by O-mannosyl glycans, which are short linear oligosaccharides consisting of one to five mannose residues (12), causes the proteins to adopt rod-like structures to span the periplasmic space and interact directly with the cell wall (36, 44, 46).

We show here that O mannosylation of these domains is not only a structurally important modification but in fact is crucial for the stability of Wsc proteins and Mid2p. O-Mannosyl glycans protect the extracellular N-terminal regions of the type I plasma membrane sensors from incorrect processing and thereby ensure signaling competency. Several lines of evidence support this finding. First, the Wsc proteins Wsc1p and Wsc2p are less extensively O mannosylated in *pmt* mutants, as deduced from the decrease in molecular mass of those glycoproteins compared to the wild type (Fig. 4). In addition, and even more strikingly, the total amount of the O-mannosylated forms of Wsc1p and Wsc2p is dramatically reduced, most notably in *pmt2 pmt4*Δ cells. Second, protein fragments of Wsc1p and Wsc2p with molecular masses lower than expected for the nonmannosylated proteins are present in *pmt* mutants (Fig. 4). In the case of Wsc1p^{HA} (predicted molecular mass of 44.8 kDa), fragments of <35 kDa were detected, whose masses are very similar to those observed for a mutant version of Wsc1p from which the N-terminal domain (amino acids 22 to 244) was deleted (36). Considering that phosphorylation of the C-terminal region of Wsc1p results in slower migration in SDS-PAGE (36), the protein fragments might be even smaller than indicated by their apparent molecular masses on SDS-polyacrylamide gels. Third, analyses of N- and O-linked carbohydrate chains (Fig. 7B and 8B), pulse-chase labeling (Fig. 7C), and N-terminal sequence analyses (Fig. 8A) showed that the 47- and 40-kDa fragments of Mid2p represent truncated forms, with various degrees of O mannosylation, which originate from high-molecular-mass precursors. Because Mid2p is less glycosylated in *pmt* mutants but is still intact in the ER (Fig. 7C, and data not shown), and because the truncated forms of the protein become localized to the plasma membrane (references 30 and 46 and data not shown), incorrect processing must occur either while Mid2p is transiting through the Golgi apparatus or after it has reached the plasma membrane.

In yeast, the function of another O-mannosylated type I plasma membrane protein, Axl2p/Bud10p, is affected by the absence of O-linked glycans due to proteolytic cleavage of the protein (51). Axl2p is required for the axial budding pattern of haploid cells. O-linked glycosylation increases Axl2p activity by enhancing the protein's stability and promoting its localization to the plasma membrane. In *pmt4*Δ mutants, the N-terminal Ser/Thr-rich region is removed while Axl2p transits the Golgi apparatus. A similar degradation pathway might apply to Wsc proteins and Mid2p.

Several members of the PMT family contribute to the O mannosylation of Wsc1p, Wsc2p, and Mid2p. We show here that Wsc1p, Wsc2p, and Mid2p are O mannosylated by, at least, Pmt2p and Pmt4p (Fig. 4 to 8). In an earlier study, it was suggested that Mid2p is O mannosylated exclusively by Pmt2p

and that Wsc1p is not a Pmt2p substrate (44). These apparent discrepancies can be explained by differences in experimental design. We analyzed Wsc1p and Mid2p expressed on single- and multicopy plasmids in different *pmt* mutants, whereas Philip and Levin only studied O mannosylation of overexpressed versions of Mid2p and Wsc1p (44). We could show that overexpression of Mid2p and Wsc1p in *pmt* mutants brings about an increase in the amount of high-molecular-mass protein variants (Fig. 6A and data not shown). These observations are in agreement with our finding that a lack of O mannosylation causes aberrant protein processing. Upon overexpression, large amounts of underglycosylated forms of Mid2p and Wsc1p arise, which in part might escape proteolytic processing. Therefore, in our biochemical analyses we focused on single-copy versions of the Wsc proteins and Mid2p. Even there it became obvious that a fraction of the proteins escaped processing (Fig. 4, 6, and 7). Thus, we attached great importance to detect both qualitative and quantitative changes in the Western blot analyses.

In the *pmt2 pmt4Δ* mutant, protein variants of Wsc1p and Mid2p that are still O mannosylated could be detected (Fig. 4A and 6A and data not shown), indicating that Wsc1p and Mid2p are also substrates for other O-mannosyltransferases. One of these appears to be Pmt1p, which forms a heteromeric complex with Pmt2p (17) and which restores glycosylation of Wsc1p when overexpressed in *pmt2 pmt4Δ* cells (Fig. 5). Wsc1p is also less highly glycosylated when isolated from a *pmt1Δ* mutant strain (data not shown). Glycosylation of Mid2p is affected in both *pmt2Δ* and *pmt1Δ* mutants, but the effect in *pmt1Δ* mutants is less pronounced, and overexpression of Pmt1p in *pmt2 pmt4Δ* mutants does not obviously affect Mid2p maturation (data not shown). In addition, Pmt3p is also capable of O-mannosylating Wsc1p in vivo, because Wsc1p shows a further decrease in glycosylation in a *pmt2 pmt3Δ* mutant compared to a *pmt2Δ* strain (data not shown).

O mannosylation is initiated by PMT family members as their substrate proteins enter the ER (52). Typical substrates of PMTs contain Ser/Thr-rich domains that, as a rule, are mannosylated by more than one PMT family member. This is the case for the cell wall proteins Cts1p (13) and Cw5p (10), the Golgi protease Kex2p (14), the plasma membrane protein Axl2p (51), and, as shown here, WSC family members and Mid2p. The only known exception is mutant α -factor precursor, which is O mannosylated exclusively by Pmt2p (21). However, mutant α -factor precursor lacks a Ser/Thr-rich domain and is O mannosylated only because its exit from the ER is slowed.

Cell wall perturbations in *pmt* mutants result in activation of the PKC1-MPK1-dependent cell wall compensatory mechanism. The cell wall is an essential structure in yeast (31). It is composed of β -glucan (~50% of cell wall dry mass), mannoproteins (~50%), and chitin (~2%). Cell wall perturbations induced in yeast cells by treatment with cell wall-destabilizing agents and by mutations in genes involved in cell wall biogenesis cause the activation of the PKC1-MPK1-dependent cell wall compensatory mechanism (9, 32). This compensates for cell wall weakening by, for instance, increasing the chitin content of the cell wall (45). The majority of cell wall mannoproteins are both N glycosylated and highly O mannosylated (52). In N-glycosylation mutants, which lead to a truncation of the

mannan structure on cell wall proteins, the PKC1-MPK1-dependent cell wall compensatory mechanism is activated (32). Similarly, a decrease in the amount of O-linked sugars will globally affect cell wall mannoproteins (41, 52), which in turn might cause cell wall perturbations and induce the PKC1-MPK1-dependent cell wall compensatory mechanism. Consistent with this, a basal activation of the cell integrity pathway occurs in *pmt2 pmt4Δ* cells, as indicated by a constitutively increased level of Mpk1p phosphorylation (Fig. 2). A PKC1 pathway-dependent reporter (*PIR3-lacZ*) confirmed these results. *PIR3* encodes a covalently linked cell wall protein (41), and its expression is increased in response to activation of Mpk1 (27). In comparison to that in wild-type yeast, *PIR3*-dependent transcription is elevated significantly in *pmt* single mutants and more strongly still in *pmt* double mutants (data not shown). In addition, the cell wall chitin content is significantly increased in *pmt* mutants (13).

In *pmt2 pmt4Δ* mutants the PKC1 pathway is not activated in response to mating pheromone (Fig. 2) or heat stress (data not shown), highly likely due to impaired signaling through the plasma membrane sensors of the WSC family and Mid2p. However, in *pmt2 pmt4Δ* cells, the PKC1-MPK1-dependent cell wall compensatory mechanism is activated (see above), suggesting that Wsc proteins and Mid2p are not required for this response. It remains to be elucidated how global cell wall perturbations are sensed in *pmt* mutants. In mannose-utilizing protein glycosylation mutants, *SHO1*-dependent activation of a *STE12* signaling pathway occurs (7), and this pathway is also induced in *pmt* mutants (U. Schermer and S. Strahl, unpublished data). Recently, a connection between the Cdc42 GTPase and the MPK1-mediated cell integrity pathway was shown (48), suggesting that in yeast cross talk between different MAP kinase pathways might contribute to the activation of cell wall compensatory mechanisms.

Why is protein O mannosylation vital? *wsc1 mid2Δ*, *wsc1 wsc2 wsc3 wsc4Δ*, and *pkc1Δ* mutants are viable when osmotically stabilized (44, 56, 59). Thus, loss of function of the type I plasma membrane sensors of the PKC1 pathway explains why *pmt2 pmt4Δ* mutants are osmolabile but not why the additional deletion of *PMT1* causes cell death of *pmt1 pmt2 pmt4Δ* mutants (13). In *pmt2 pmt4Δ* mutant cells, not only Wsc proteins and Mid2p but many other plasma membrane and cell wall proteins will be affected (51, 52). This results in a generally weakened cell wall, and compensatory mechanisms are necessary to stabilize cells. Once the O-mannosylating capacity falls below a critical level, the folding, maturation, and/or stability of too many glycoproteins might be perturbed for the cells to be able to compensate for all of these defects.

ACKNOWLEDGMENTS

We thank C. Endres and M. Priesmeier-Grädler for excellent technical assistance, C. Frank, and T. Schäfer for providing assistance with the construction of plasmids, and U. Schermer for assistance with *PIR3*-dependent transcription. We thank R. Gerstl for assistance in purification of Mid2p^{ProtA} and R. Deutzmann for N-terminal protein sequence analyses. We are grateful to R. Ballester, H. Bussey, J. Heinisch, D. Levin, L. Lehle, J. Stolz, and T. Willer for generously providing plasmids or antibodies. We thank W. Tanner for many helpful discussions and generous support and P. Orlean and J. Stolz for critical reading of the manuscript.

The Deutsche Forschungsgemeinschaft (grant SFB521) supported this work.

REFERENCES

- Ballard, M. J., W. A. Tyndall, J. M. Shingle, D. J. Hall, and E. Winter. 1991. Tyrosine phosphorylation of a yeast 40 kDa protein occurs in response to mating pheromone. *EMBO J.* **10**:3753–3758.
- Beltran-Valero De Bernabe, D., S. Currier, A. Steinbrecher, J. Celli, E. Van Beusekom, B. Van Der Zwaag, H. Kayserili, L. Merlini, D. Chitayat, W. B. Dobyns, B. Cormand, A. E. Lehesjoki, J. Cruces, T. Voit, C. A. Walsh, H. Van Bokhoven, and H. G. Brunner. 2002. Mutations in the O-mannosyltransferase gene POMT1 give rise to the severe neuronal migration disorder Walker-Warburg syndrome. *Am. J. Hum. Genet.* **71**:1033–1043.
- Bickle, M., P. A. Delley, A. Schmidt, and M. N. Hall. 1998. Cell wall integrity modulates RHO1 activity via the exchange factor ROM2. *EMBO J.* **17**:2235–2245.
- Buehrer, B. M., and B. Errede. 1997. Coordination of the mating and cell integrity mitogen-activated protein kinase pathways in *Saccharomyces cerevisiae*. *Mol. Cell. Biol.* **17**:6517–6525.
- Christianson, T. W., R. S. Sikorski, M. Dante, J. H. Shero, and P. Hieter. 1992. Multifunctional yeast high-copy-number shuttle vectors. *Gene* **110**:119–122.
- Costigan, C., S. Gehrung, and M. Snyder. 1992. A synthetic lethal screen identifies SLK1, a novel protein kinase homolog implicated in yeast cell morphogenesis and cell growth. *Mol. Cell. Biol.* **12**:1162–1178.
- Cullen, P. J., J. Schultz, J. Horecka, B. J. Stevenson, Y. Jigami, and G. F. Sprague, Jr. 2000. Defects in protein glycosylation cause SHO1-dependent activation of a STE12 signaling pathway in yeast. *Genetics* **155**:1005–1018.
- Delley, P. A., and M. N. Hall. 1999. Cell wall stress depolarizes cell growth via hyperactivation of RHO1. *J. Cell Biol.* **147**:163–174.
- de Nobel, H., C. Ruiz, H. Martin, W. Morris, S. Brul, M. Molina, and F. M. Klis. 2000. Cell wall perturbation in yeast results in dual phosphorylation of the Slr2/Mpk1 MAP kinase and in a Slr2-mediated increase in FKS2-lacZ expression, glucanase resistance and thermotolerance. *Microbiology* **146**:2121–2132.
- Ecker, M., V. Mersa, I. Hagen, R. Deutzmann, S. Strahl, and W. Tanner. 2003. O-mannosylation precedes and potentially controls N-glycosylation of a yeast cell wall glycoprotein. *EMBO Rep.* **4**:628–632.
- Gartner, A., K. Nasmyth, and G. Ammerer. 1992. Signal transduction in *Saccharomyces cerevisiae* requires tyrosine and threonine phosphorylation of FUS3 and KSS1. *Genes Dev.* **6**:1280–1292.
- Gemmill, T. R., and R. B. Trimble. 1999. Overview of N- and O-linked oligosaccharide structures found in various yeast species. *Biochim. Biophys. Acta* **1426**:227–237.
- Gentsch, M., and W. Tanner. 1996. The PMT gene family: protein O-glycosylation in *Saccharomyces cerevisiae* is vital. *EMBO J.* **15**:5752–5759.
- Gentsch, M., and W. Tanner. 1997. Protein-O-glycosylation in yeast: protein-specific mannosyltransferases. *Glycobiology* **7**:481–486.
- Gietz, D., A. St. Jean, R. A. Woods, and R. H. Schiestl. 1992. Improved method for high efficiency transformation of intact yeast cells. *Nucleic Acids Res.* **20**:1425.
- Girrbach, V., and S. Strahl. 2003. Members of the evolutionarily conserved PMT family of protein O-mannosyltransferases form distinct protein complexes among themselves. *J. Biol. Chem.* **278**:12554–12562.
- Girrbach, V., T. Zeller, M. Priesmeier, and S. Strahl-Bolsinger. 2000. Structure-function analysis of the dicholyl phosphate-mannose: protein O-mannosyltransferase ScPmt1p. *J. Biol. Chem.* **275**:19288–19296.
- Graham, T. R., and S. D. Emr. 1991. Compartmental organization of Golgi-specific protein modification and vacuolar protein sorting events defined in a yeast sec18 (NSF) mutant. *J. Cell Biol.* **114**:207–218.
- Gray, J. V., J. P. Ogas, Y. Kamada, M. Stone, D. E. Levin, and I. Herskowitz. 1997. A role for the Pkc1 MAP kinase pathway of *Saccharomyces cerevisiae* in bud emergence and identification of a putative upstream regulator. *EMBO J.* **16**:4924–4937.
- Harlow, E., and D. Lane. 1988. Antibodies: a laboratory manual. Cold Spring Harbor Laboratory Press, Cold Spring Harbor, N.Y.
- Harty, C., S. Strahl, and K. Romisch. 2001. O-mannosylation protects mutant alpha-factor precursor from endoplasmic reticulum-associated degradation. *Mol. Biol. Cell* **12**:1093–1101.
- Heinisch, J. J., A. Lorberg, H. P. Schmitz, and J. J. Jacoby. 1999. The protein kinase C-mediated MAP kinase pathway involved in the maintenance of cellular integrity in *Saccharomyces cerevisiae*. *Mol. Microbiol.* **32**:671–680.
- Hill, J. E., A. M. Myers, T. J. Koerner, and A. Tzagoloff. 1986. Yeast/*E. coli* shuttle vectors with multiple unique restriction sites. *Yeast* **2**:163–167.
- Immervoll, T., M. Gentsch, and W. Tanner. 1995. PMT3 and PMT4, two new members of the protein-O-mannosyltransferase gene family of *Saccharomyces cerevisiae*. *Yeast* **11**:1345–1351.
- Irie, K., M. Takase, K. S. Lee, D. E. Levin, H. Araki, K. Matsumoto, and Y. Oshima. 1993. *MKK1* and *MKK2*, which encode *Saccharomyces cerevisiae* mitogen-activated protein kinase-kinase homologs, function in the pathway mediated by protein kinase C. *Mol. Cell. Biol.* **13**:3076–3083.
- Jacoby, J. J., S. M. Nilius, and J. J. Heinisch. 1998. A screen for upstream components of the yeast protein kinase C signal transduction pathway identifies the product of the SLG1 gene. *Mol. Gen. Genet.* **258**:148–155.
- Jung, U. S., and D. E. Levin. 1999. Genome-wide analysis of gene expression regulated by the yeast cell wall integrity signalling pathway. *Mol. Microbiol.* **34**:1049–1057.
- Jurado, L. A., A. Coloma, and J. Cruces. 1999. Identification of a human homolog of the *Drosophila* rotated abdomen gene (POMT1) encoding a putative protein O-mannosyl-transferase, and assignment to human chromosome 9q34.1. *Genomics* **58**:171–180.
- Kaiser, C. A., S. Michaelis, and A. Mitchell. 1994. Methods in yeast genetics: a Cold Spring Harbor Laboratory course manual. Cold Spring Harbor Laboratory Press, Cold Spring Harbor, N.Y.
- Ketela, T., R. Green, and H. Bussey. 1999. *Saccharomyces cerevisiae* Mid2p is a potential cell wall stress sensor and upstream activator of the PKC1-MPK1 cell integrity pathway. *J. Bacteriol.* **181**:3330–3340.
- Klis, F. M., P. Mol, K. Hellingwerf, and S. Brul. 2002. Dynamics of cell wall structure in *Saccharomyces cerevisiae*. *FEMS Microbiol. Rev.* **26**:239–256.
- Lagorce, A., N. C. Hauser, D. Labourdette, C. Rodriguez, H. Martin-Yken, J. Arroyo, J. D. Hoheisel, and J. Francois. 2003. Genome-wide analysis of the response to cell wall mutations in the yeast *Saccharomyces cerevisiae*. *J. Biol. Chem.* **278**:20345–20357.
- Lee, K. S., K. Irie, Y. Gotoh, Y. Watanabe, H. Araki, E. Nishida, K. Matsumoto, and D. E. Levin. 1993. A yeast mitogen-activated protein kinase homolog (Mpk1p) mediates signalling by protein kinase C. *Mol. Cell. Biol.* **13**:3067–3075.
- Lee, K. S., and D. E. Levin. 1992. Dominant mutations in a gene encoding a putative protein kinase (BCK1) bypass the requirement for a *Saccharomyces cerevisiae* protein kinase C homolog. *Mol. Cell. Biol.* **12**:172–182.
- Levin, D. E., and E. Bartlett-Heubusch. 1992. Mutants in the *S. cerevisiae* PKC1 gene display a cell cycle-specific osmotic stability defect. *J. Cell Biol.* **116**:1221–1229.
- Lodder, A. L., T. K. Lee, and R. Ballester. 1999. Characterization of the Wsc1 protein, a putative receptor in the stress response of *Saccharomyces cerevisiae*. *Genetics* **152**:1487–1499.
- Lussier, M., M. Gentsch, A. M. Sdicu, H. Bussey, and W. Tanner. 1995. Protein O-glycosylation in yeast. The PMT2 gene specifies a second protein O-mannosyltransferase that functions in addition to the PMT1-encoded activity. *J. Biol. Chem.* **270**:2770–2775.
- Martin-Blanco, E., and A. Garcia-Bellido. 1996. Mutations in the rotated abdomen locus affect muscle development and reveal an intrinsic asymmetry in *Drosophila*. *Proc. Natl. Acad. Sci. USA* **93**:6048–6052.
- Maudrell, K. 1990. nmt1 of fission yeast. A highly transcribed gene completely repressed by thiamine. *J. Biol. Chem.* **265**:10857–10864.
- Mazzoni, C., P. Zarov, A. Rambourg, and C. Mann. 1993. The SLT2 (MPK1) MAP kinase homolog is involved in polarized cell growth in *Saccharomyces cerevisiae*. *J. Cell Biol.* **123**:1821–1833.
- Mrsa, V., T. Seidl, M. Gentsch, and W. Tanner. 1997. Specific labelling of cell wall proteins by biotinylation. Identification of four covalently linked O-mannosylated proteins of *Saccharomyces cerevisiae*. *Yeast* **13**:1145–1154.
- Nonaka, H., K. Tanaka, H. Hirano, T. Fujiwara, H. Kohno, M. Umikawa, A. Mino, and Y. Takai. 1995. A downstream target of RHO1 small GTP-binding protein is PKC1, a homolog of protein kinase C, which leads to activation of the MAP kinase cascade in *Saccharomyces cerevisiae*. *EMBO J.* **14**:5931–5938.
- Ono, T., T. Suzuki, Y. Anraku, and H. Iida. 1994. The MID2 gene encodes a putative integral membrane protein with a Ca(2+)-binding domain and shows mating pheromone-stimulated expression in *Saccharomyces cerevisiae*. *Gene* **151**:203–208.
- Philip, B., and D. E. Levin. 2001. Wsc1 and Mid2 are cell surface sensors for cell wall integrity signaling that act through Rom2, a guanine nucleotide exchange factor for Rho1. *Mol. Cell. Biol.* **21**:271–280.
- Popolo, L., T. Gualtieri, and E. Ragni. 2001. The yeast cell-wall salvage pathway. *Med. Mycol.* **39**(Suppl. 1):111–121.
- Rajavel, M., B. Philip, B. M. Buehrer, B. Errede, and D. E. Levin. 1999. Mid2 is a putative sensor for cell integrity signaling in *Saccharomyces cerevisiae*. *Mol. Cell. Biol.* **19**:3969–3976.
- Robinson, J. S., D. J. Klionsky, L. M. Banta, and S. D. Emr. 1988. Protein sorting in *Saccharomyces cerevisiae*: isolation of mutants defective in the delivery and processing of multiple vacuolar hydrolases. *Mol. Cell. Biol.* **8**:4936–4948.
- Rodriguez-Pachon, J. M., H. Martin, G. North, R. Rotger, C. Nombela, and M. Molina. 2002. A novel connection between the yeast Cdc42 GTPase and the Slr2-mediated cell integrity pathway identified through the effect of secreted *Salmonella* GTPase modulators. *J. Biol. Chem.* **277**:27094–27102.
- Rose, A. H. 1975. Growth and handling of yeasts. *Methods Cell Biol.* **12**:1–16.
- Sambrook, J., E. F. Fritsch, and T. Maniatis. 1989. Molecular cloning: a laboratory manual, 2nd ed. Cold Spring Harbor Laboratory Press, Cold Spring Harbor, N.Y.
- Sanders, S. L., M. Gentsch, W. Tanner, and I. Herskowitz. 1999. O-glycosylation of Axl2/Bud10p by Pmt4p is required for its stability, localization, and function in daughter cells. *J. Cell Biol.* **145**:1177–1188.
- Strahl-Bolsinger, S., M. Gentsch, and W. Tanner. 1999. Protein O-mannosylation. *Biochim. Biophys. Acta* **1426**:297–307.
- Strahl-Bolsinger, S., and A. Scheinost. 1999. Transmembrane topology of

- Pmt1p, a member of an evolutionarily conserved family of protein O-mannosyltransferases. *J. Biol. Chem.* **274**:9068–9075.
54. **te Heesen, S., B. Janetzky, L. Lehle, and M. Aebi.** 1992. The yeast WBP1 is essential for oligosaccharyl transferase activity in vivo and in vitro. *EMBO J.* **11**:2071–2075.
55. **Verna, J., A. Lodder, K. Lee, A. Vagts, and R. Ballester.** 1997. A family of genes required for maintenance of cell wall integrity and for the stress response in *Saccharomyces cerevisiae*. *Proc. Natl. Acad. Sci. USA* **94**:13804–13809.
56. **Watanabe, M., C. Y. Chen, and D. E. Levin.** 1994. *Saccharomyces cerevisiae* PKC1 encodes a protein kinase C (PKC) homolog with a substrate specificity similar to that of mammalian PKC. *J. Biol. Chem.* **269**:16829–16836.
57. **Willer, T., W. Amselgruber, R. Deutzmann, and S. Strahl.** 2002. Characterization of POMT2, a novel member of the PMT protein O-mannosyltransferase family specifically localized to the acrosome of mammalian spermataids. *Glycobiology* **12**:771–783.
58. **Zarrov, P., C. Mazzoni, and C. Mann.** 1996. The SLT2 (MPK1) MAP kinase is activated during periods of polarized cell growth in yeast. *EMBO J.* **15**:83–91.
59. **Zu, T., J. Verna, and R. Ballester.** 2001. Mutations in WSC genes for putative stress receptors result in sensitivity to multiple stress conditions and impairment of Rlm1-dependent gene expression in *Saccharomyces cerevisiae*. *Mol. Genet. Genomics* **266**:142–155.